

## SHORT PERIOD GROUP VELOCITY MEASUREMENTS AND MAPS IN CENTRAL ASIA

A.L. Levshin,<sup>1</sup> M.H. Ritzwoller,<sup>1</sup> M.P. Barmin,<sup>1</sup> and J.L. Stevens<sup>2</sup>

University of Colorado at Boulder,<sup>1</sup> Science Applications International Corporation<sup>2</sup>

Sponsored by Defense Threat Reduction Agency

Contract No. DTRA01-00-C-0026

### **ABSTRACT**

The purpose of this study is to improve group velocity maps designed to advance the detection and discrimination capabilities for the area encompassed by western China, northern India, and Pakistan. These maps may be used to construct sharply tuned phase-matched filters for extracting weak surface wave signals from background noise and to make better estimates of surface wave spectral magnitudes for small events. We are working now to obtain a greatly expanded data set of short-period measurements (7 - 15 s). We have analyzed seismograms following approximately 1,000 events that occurred in and around the studied region from 1996 - 1999. We obtained about 6,000 short-period dispersion curves for Rayleigh and 4,000 curves for Love waves. We added these measurements to existing dispersion curves and estimated a refined set of dispersion maps on a one-degree grid worldwide. Here we present preliminary refined group velocity maps from 10-s to 18-s periods. Improvements produced by the new data set are mostly at the shorter end of this period band in Central Asia.

**KEY WORDS:** Central Asia, surface waves, group velocities,  $M_s:m_b$  discriminant

### **OBJECTIVE**

The goal of this research is to improve the ability to detect and discriminate small events over wide areas of Central Asia using regional seismic data. We extend the existing set of Rayleigh and Love wave tomographic group velocity maps to periods shorter than 15 s. Accurate maps at shorter periods would improve signal detection capabilities by advancing signal-to-noise enhancement produced by phase-matched filters. This permits the extension of surface wave magnitude ( $M_s$ ) estimates to periods shorter than 15 s and to smaller events than current capabilities allow. This is the basis for future tests of  $M_s:m_b$  discriminant for these events.

### **RESEARCH ACCOMPLISHED**

#### **Introduction**

Detection, location, and identification of small seismic events all depend on calibration of source and path effects to ensure maximum efficiency of the monitoring at small magnitudes. The described research, which began in April 2000, is dedicated to advancing detection and discrimination capabilities for small magnitude events by improving calibration information for surface waves in western China, Pakistan, northern India, and surrounding areas. The calibration information will be in the form of short period (7 s - 15 s) Rayleigh and Love wave tomographic group velocity maps and station-specific correction surfaces constructed from these maps. Although we have previously provided similar information in the region of study at intermediate periods (15 s - 50 s; e.g., Stevens and McLaughlin, 1997; Ritzwoller *et al.*, 1998; Levshin *et al.*, 1998), the group velocity maps and correction surfaces at short periods are entirely new (Levshin *et al.*, 2000). This new information will be rigorously tested at the Center for Monitoring Research (CMR) Test bed to quantify the improvement in the ability to estimate surface wave amplitudes and, hence,  $M_s$  for smaller events than are currently possible.

The  $M_s:m_b$  discriminant and its regional variants are the most reliable transportable means of discriminating earthquakes from explosions (e.g., Stevens and Day, 1985, Stevens and McLaughlin, 2001). To measure surface wave amplitudes accurately in order to estimate  $M_s$  is challenging for small magnitude events in which surface waves may not be readily identifiable in raw seismograms. Because amplitude spectra of regionally recorded small magnitude events typically peak below 20-s period (where  $M_s$  is usually measured) the regional application of the  $M_s:m_b$  discriminant may be improved if  $M_s$  were measured at significantly shorter periods; i.e., 8- to 12-s period. To provide these amplitude measurements, it is crucial to be able to reliably detect small amplitude surface waves and accurately measure the corresponding spectral amplitudes. This goal may be achieved using phase-matched filters (Russell *et al.*, 1988; Herrin & Gofort, 1977; Levshin & Ritzwoller, 2001) that are tuned for all source/station paths of interest. Designing of such filters requires perfect knowledge of surface wave propagation across the regions being monitored. This is the motivation for the current efforts of University of Colorado at Boulder (CU) and SAIC seismologists to obtain new data on short-period surface wave velocities in Central Asia and surroundings. Such measurements will be used for constructing short-period group velocity maps, the refined regionalized 3D crustal model (Stevens and McLaughlin, 1997; 2001), and 2-D group velocity correction surfaces (Levshin *et al.*, 1998) needed for designing the locally tuned phase-matched filters.

CU and SAIC are working collaboratively to:

- obtain a new and vastly expanded set of group velocity measurements in the region of study emphasizing measurements between 7-s and 15-s period;
- convert these measurements into group velocity maps and station-specific correction surfaces using both tomographic and model-based methods;
- cross-validate the tomographic and model-based methods to obtain a set of maps and surfaces that are judged most reliable for the area of study;
- embed these maps and surfaces into global maps and surfaces constructed by the SAIC group;
- test and validate the new maps and corrections surfaces with a rigorous set of tests performed on regional data at the CMR Test bed; and
- deliver documentation and reports of all results with the completed maps and surfaces to customers at DOE, CMR, the U.S. National Data Center (NDC), and the International Data Centre (IDC).

The final results will be provided in a form that can be easily used within operational monitoring systems for surface wave identification and phase-matched filtering.

### **Improvement of Detection Capabilities Using Phase-Matched Filtering**

Recent work done by the SAIC group (formerly Maxwell Technologies) has focused on techniques for improving surface wave measurements and reducing the surface wave detection threshold, and, particularly, on further development of MAXSURF, the code used at the IDC and prototype IDC (PIDC) for automatic identification and measurement of surface waves. MAXSURF is responsible for all surface wave processing at the IDC and the PIDC and runs in the processing stream after events have been identified and located. Surface wave group velocity measurements provided by CU were combined with other available sets of phase and group velocity measurements and used to construct a refined set of global dispersion maps on a one-degree grid. Surface wave detection at the IDC currently compares predicted dispersion curves with measurements from seismograms such as those shown in Figure 1a. The procedure can be improved by using phase-matched filtering, which compresses the signal into a narrow time window improving the signal-to-noise ratio (Figure 1b). Phase-matched filtering requires accurate dispersion measurements at short periods, particularly for low-amplitude arrivals on short paths.

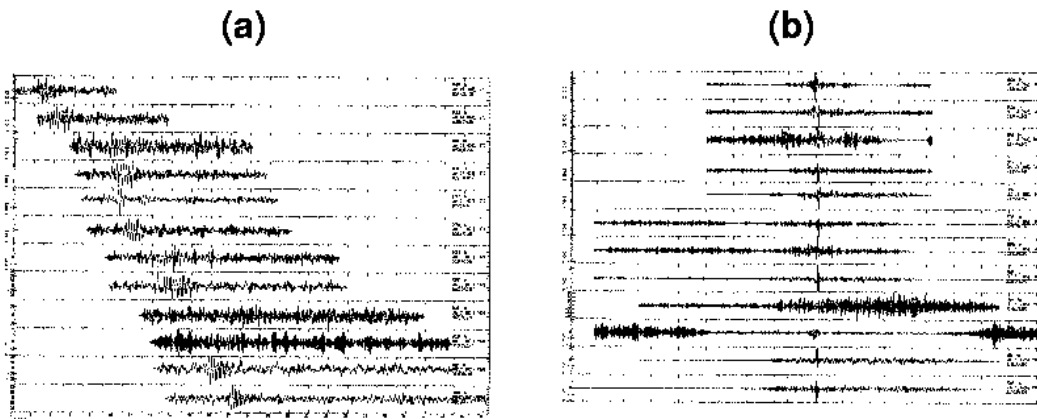


**Figure 1.** a. Surface wave data from an  $m_b$  3.9 South Pacific earthquake after transformation to a KS36000 instrument. b. Same data after phase-matched filtering.

MAXSURF then examines the arrival window where a surface wave would be expected and applies a dispersion test to see if a surface wave can be identified. If so, then the amplitude is measured and stored in the IDC database. Surface waves are identified in the following way. A set of narrow-band filters is applied to the data over a set of eight periods from 16 s to 50 s. A long-period or broadband beam is formed at arrays with the expected azimuth and slowness. The arrival times at each frequency are then compared with predicted arrival times generated from the regionalized group velocity model (Figure 2a). The efficiency of detection depends on the accuracy. To improve detection, we apply phase-matched filtering first; then we apply narrow-band filters.

### Detection Using Phase-Matched Filtering and Narrow-Band Filtering

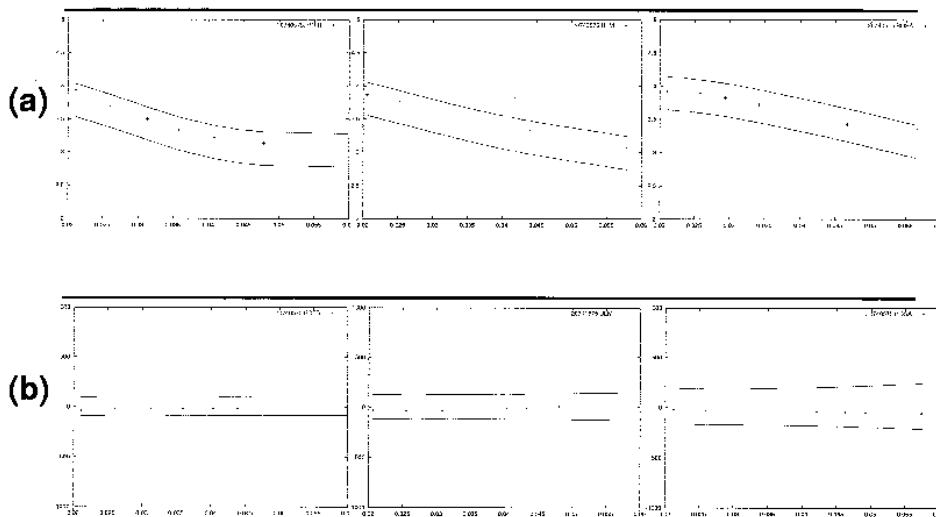


**Figure 2.** a. Narrow-band filter detection compares measured group velocity with the regionalized model. Measured dispersion data for an  $m_b$  4.2 earthquake observed at 3 stations are shown. b. To improve detection, the data are phase-match filtered, then they are passed through narrow-band filters. The detection test is applied for the same time interval, but the time is now centered around zero.

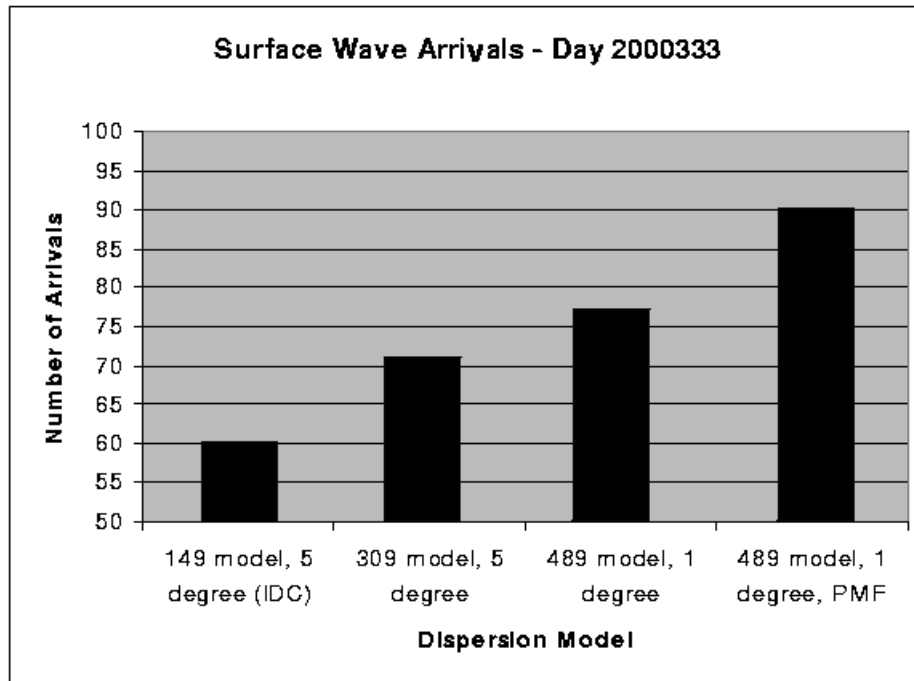


**Figure 3.** Improvement in the number of detections for a day of data with improvements in the model, and with phase matched filtering.

The number of detections increased by 32% over current IDC detections with phase-matched filtering using the most recent one-degree model. The detection test is applied for the same time interval but the time now is centered around zero (Figure 2b). Improvement in the number of detections for a day using the more detailed ( $1^\circ \times 1^\circ$ ) model and phase-matched filtering (PMF) is demonstrated in Figure 3. The number of detections increased by 32% over current IDC detections with phase-matched filtering using the most recent one-degree model.

This example demonstrates the importance of good group velocity maps. Because surface waves are identified by comparison with predicted arrival times, it is essential that the predicted group velocities are accurate. One way to reduce the threshold further is to increase the frequency band over which surface waves can be measured. The current band of 16-s to 50-s period was found to be a good band for worldwide surface wave data measured at distances of 20-100 degrees, and the global dispersion maps are fairly well defined over this period band. However, at shorter distances, surface waves are dominated by higher frequencies. To improve signal-to-noise ratio and to measure surface waves at close range, the dispersion test and measurement of surface waves should be performed at higher frequencies.

### Data and Measurements

*Data acquisition.* We acquired waveform data from IRIS DMC, GEOSCOPE, and GEOFON data centers for the seismic events that occurred in 1996-1999. Data from 850 events recorded by about 90 stations of the GSN, GEOSCOPE, KNET, KAZNET, CDSN, and GEOFON networks have been obtained. We combined these data with relevant data collected in our previous studies of this region (Levshin & Ritzwoller, 2001). Figure 4 shows positions of stations and events used in this study. Further acquisition of data is in progress.

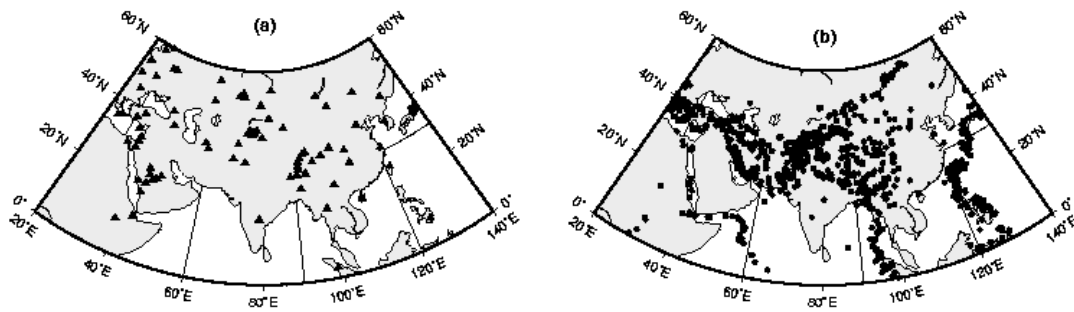


**Figure 4.** Station and event locations. a. The location of seismic stations used in this study (triangles); b. The locations of the events (circles).

*Data processing.* All data and corresponding event and station information were converted into CSS3.0 formatted event volumes and processed by seismic analysts in a semi-automatic regime using the frequency-time analysis package developed at CU. We used the Frequency-Time Analysis (FTAN) method (e.g., Dziewonski *et al.*, 1968; Levshin *et al.*, 1972; Russell *et al.*, 1988; Levshin *et al.*, 1992; Ritzwoller *et al.*, 1995) to obtain group and phase velocity, and spectral amplitude measurements. As part of FTAN, an analyst interactively designed a group velocity-period filter to reduce contamination from other waves and coda, chose the frequency band for each measurement, and assigned a qualitative grade (A - F) to each measurement. All resulting measurements of group velocities and other surface wave characteristics were preserved in a format that is an extension of the CSS3.0 format. Altogether, more than 6,000 dispersion curves of Rayleigh waves and 4,000 dispersion curves of Love waves were obtained. An example of successful measurements is shown in Figure 5. The event occurred on 8/26/1999 in southeastern Afghanistan with  $m_b = 5.2$  and  $M_s = 4.4$ . Presence of strong higher modes and multiple arrivals interfering with the fundamental modes makes some measurements problematic (Figure 6). Further data processing included data cleaning based on comparison of observed travel times with those predicted by the CU Eurasian model (Villaseñor *et al.*, 2001), and *declustering*, i.e. combining data from very close paths in a single observation (Ritzwoller & Levshin, 1998). These procedures reduce the number of paths used in tomographic inversion by approximately a factor of two.

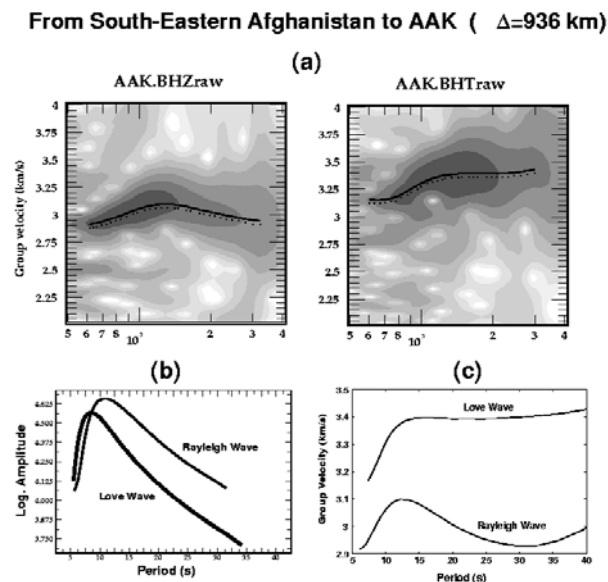


**Figure 5.** Example of successful short-period measurements: a. Raw FTAN diagrams for Rayleigh and Love waves; b. Spectral amplitude curves of Rayleigh and Love waves; c. Group velocities.

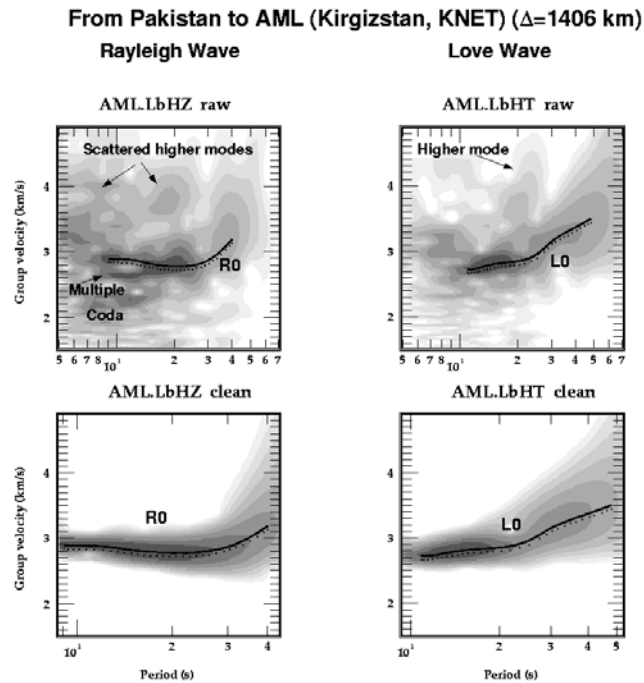


**Figure 6.** Example of difficulties met in making short-period measurements due to interference with higher modes and multiple arrivals: a. Raw FTAN diagrams for Rayleigh and Love waves; b. Clean FTAN diagrams.

*Data coverage.* Figure 7 contrasts path density at periods of 10 s, 14 s, and 18 s for our existing data set. Path densities at 14 s and 18 s are much better than at 10 s, partially because at and above 14-s period, measurements can be obtained for paths significantly longer than 2,000 km. Path density for Love waves is significantly less than for Rayleigh waves, mostly due to lower signal-to-noise ratio at the horizontal components and unresolvable interference with Rayleigh waves due to off-path propagation. The densest coverage at short periods is observed around KNET.

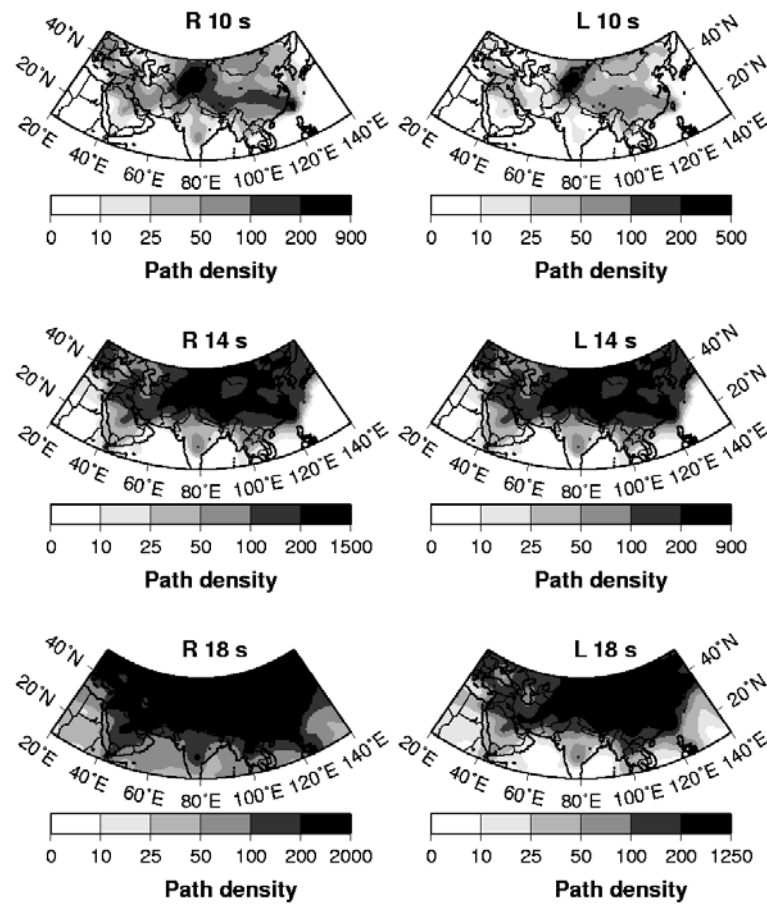


**Figure 7.** Path density for the current Rayleigh wave (left column) and Love wave (right column) data set at 10 s, 14 s, and 18 s periods. Units are number of paths intersecting each  $2^{\circ} \times 2^{\circ}$  cell ( $50,000 \text{ km}^2$ ).

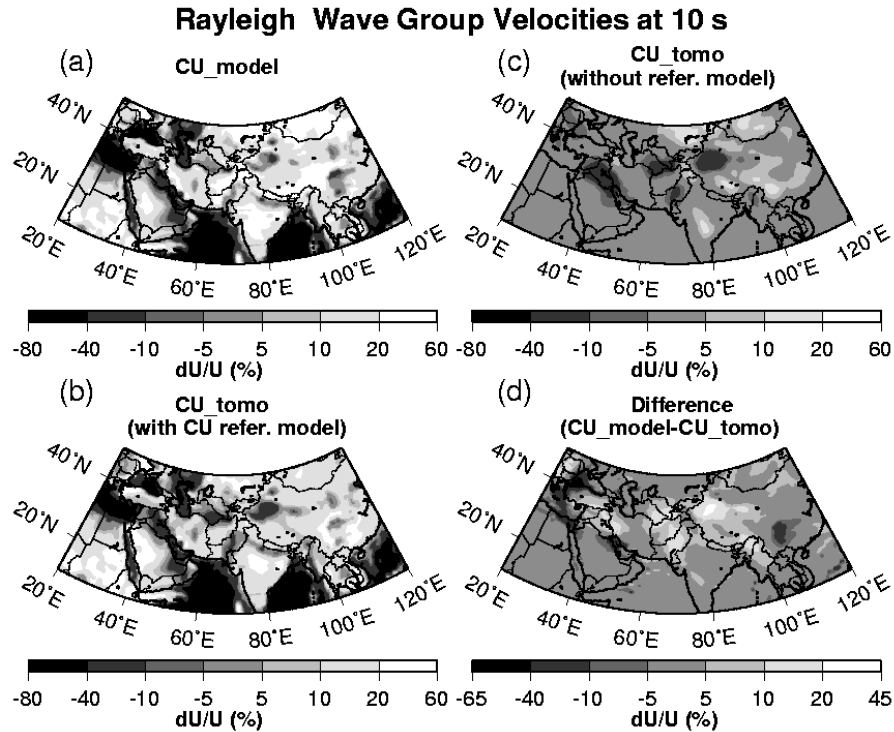


**Figure 8.** Rayleigh wave group velocities at 10 s. a. Reference map predicted by the CU model; b. Tomographic map obtained using reference map (a); c. Tomographic map obtained without use of reference map; d. Difference between prediction (a) and result (b).

### Tomographic Inversion

*Method.* Our tomographic method is described in (Barmin *et al.*, 2001). At each period, we estimate a group velocity perturbation,  $\delta U(\theta, \phi)$ , relative to a reference map,  $U_o(\theta, \phi)$

which itself may be spatially variable so that group velocity at each spatial point  $(\theta, \phi)$  is

$$U(\theta, \phi) = U_o(\theta, \phi) + \delta U(\theta, \phi)$$

We use our recent CU model (Villaseñor *et al.*, 2001) to compute the reference map. We construct  $\delta U(\theta, \phi)$  by minimizing the weighted misfit to the data together with both spatial smoothing and model norm regularization constraints. The spatial smoothing constraint determines the wavenumber content of the estimated map. For data that are inhomogeneously distributed, the model norm constraint is very important, and we use path density to determine the strength of this constraint. Where path density is very low (e.g., in southern India at 10 s in Figure 6),  $\delta U(\theta, \phi)$  will be strongly damped and constrained to equal the reference model.



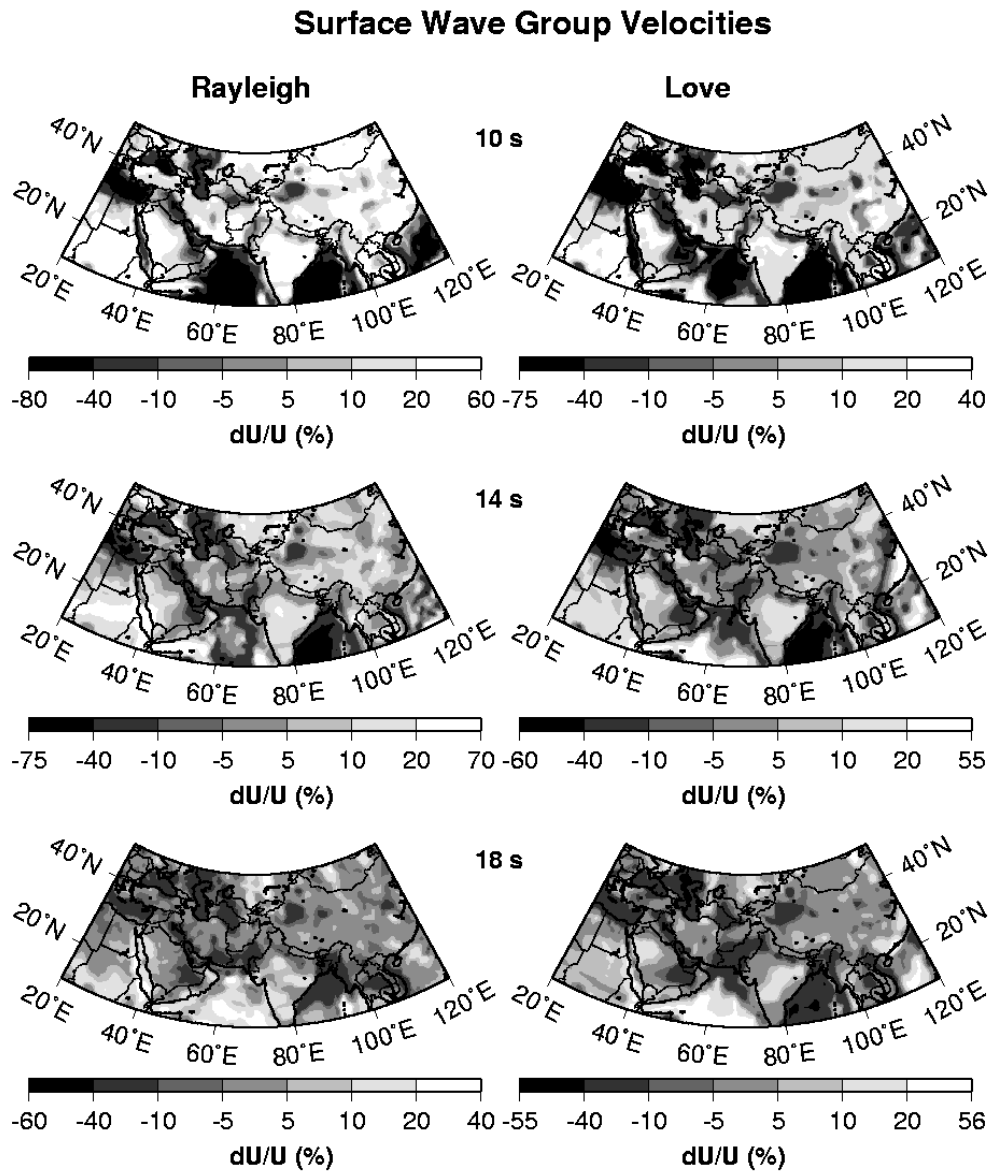


**Figure 9.** a. Group velocity maps for Rayleigh and Love waves at 8 and 10 s. b. Group velocity maps for Rayleigh and Love waves at 14 and 18 s.

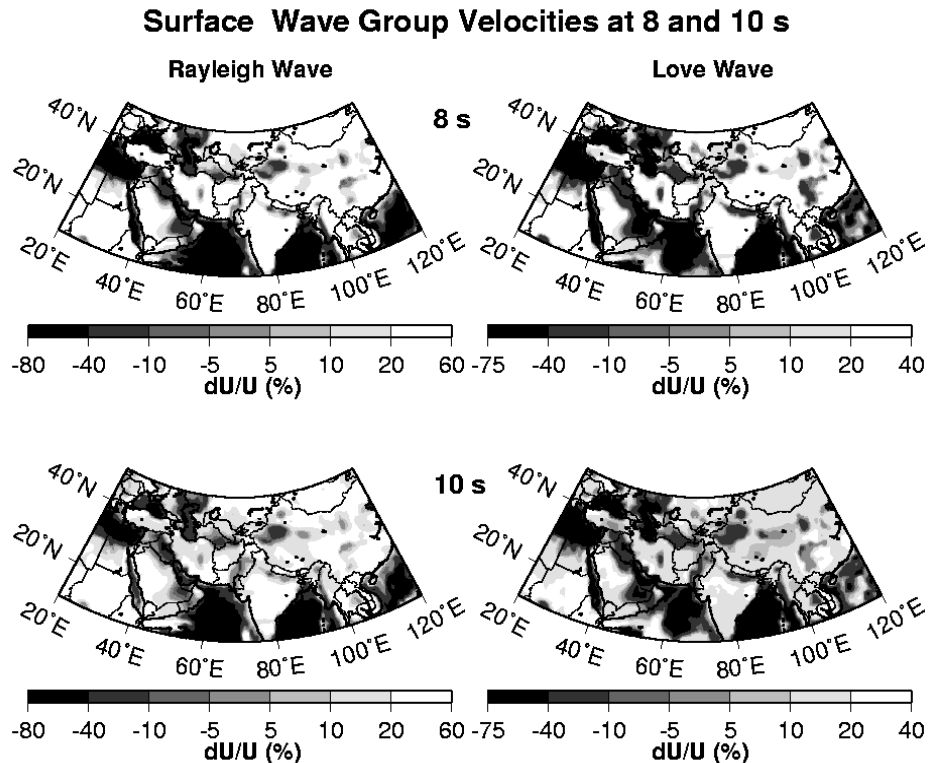


**Figure 10.** Preliminary tomographic maps.

Tomographic maps for a set of short periods obtained using the current data set are shown in Figures 8 and 9. The important role of the reference model is clearly demonstrated by Figure 8. Map (a) presents the prediction from the CU model. Map (b) shows the results of tomography with Map (a) as a reference. Map (c) presents results of tomographic inversion without the reference model. In this case, a mean value of observed group velocities was taken as a reference value across the mapped area. Map (d) shows the relative difference between maps (a) and (b). At first glance, there is no significant difference between maps (a) and (b), and this suggests that tomography does not produce significant new information about the studied area. However, map (c) shows that the data contain signals which could be informative, and map (d) demonstrates significant differences between the prediction and the result of tomography in areas with good path coverage. For example, the low-velocity feature related to the Tarim basin around point  $\theta = 80^\circ$ ,  $\phi = 38^\circ$ , is much more prominent than in the model prediction. Another feature that is almost absent in the prediction is a low-velocity spot in eastern Pakistan at periods 12 s and above. At the same time, group velocities in areas with poor coverage (like southern India, northeastern Africa) tend to be almost the same as in the reference model. Tomographic maps for four different periods (8, 10, 14, and 18 s) are shown in Figure 9. Sedimentary basins of the Tarim, Dzhungaria, Caspian, Black, and Mediterranean Seas are clearly seen on all maps. Low velocity regions in Pakistan are especially prominent on the 14-s maps. High-velocity regions in Iran, southeastern China and northern India appear on the 8-s, 10-s and 14-s maps. The data fit to tomographic images is two to three times better than to the predictions based on the CU model. This indicates that upper crustal structure in the CU model for this region may be refined using the short-period information obtained in this study. The same is true for the SAIC regionalized model. The values of the group velocity RMS for periods between 10 and 18 s are on the order 0.1 km/s, and the travel time RMS on the order of 20 s.

*Resolution and bias.* Some means to estimate the quality of group velocity maps are discussed at length by Barmin *et al.* (2001). Two of the most useful qualitative measures are spatially variable resolution and amplitude bias. Figure 10 presents spatial resolution and amplitude bias of the maps in Figure 9 and contrasts the 10-s and 14-s maps with respect to these measures of map quality. Resolution at 10 s is on the order of 200-350 km to the north of latitude  $25^\circ$  and

deteriorates to the south. The amplitude bias in the area with acceptable resolution is less than 20%. The resolution and amplitude bias of the 14 s maps are better than at 10 s due to the more dense coverage.

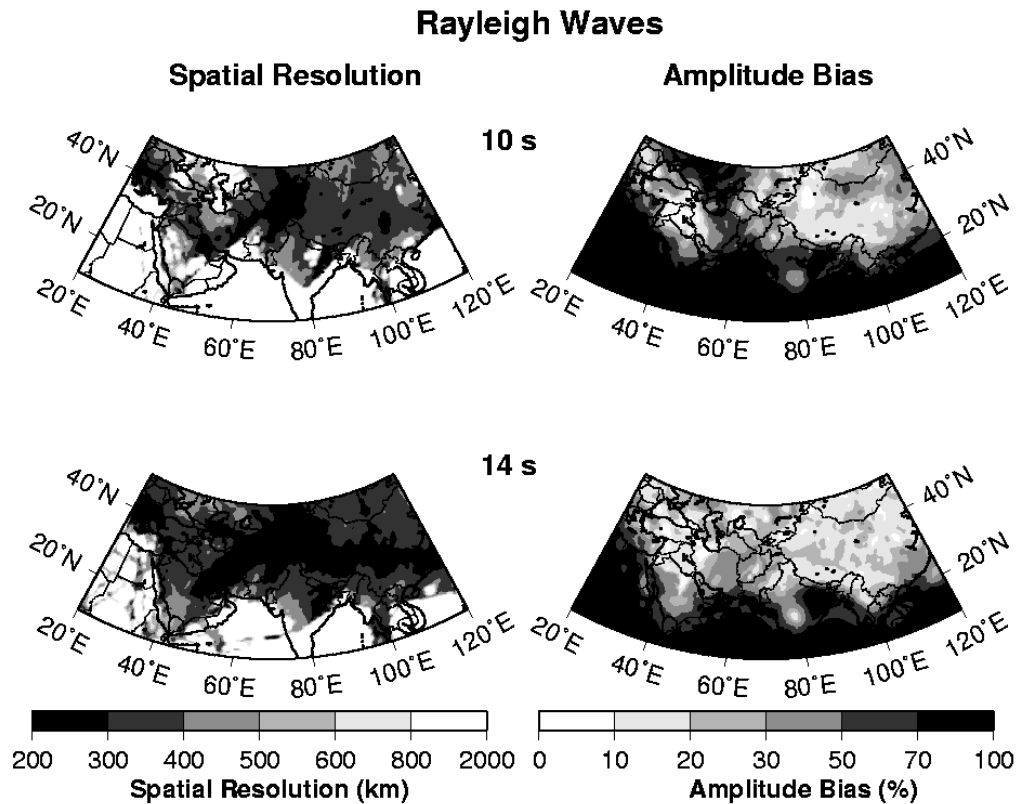


**Figure 11.** Spatial resolution and amplitude bias of tomographic inversion for the 10-s and 14-s Rayleigh wave data.

### **CONCLUSIONS AND RECOMMENDATIONS**

In future work, we plan to

- Acquire additional data and obtain additional group velocity measurements for about 250 events that occurred in 2000.
- Produce refined Rayleigh and Love wave group velocity maps in increments of 1 s from 8-s to 15-s periods for the region of study by the tomographic method.
- Convert the group velocity maps to station-specific correction surfaces for IMS and other interesting stations in and adjacent to the region of study.
- Incorporate the group velocity measurements into new global group velocity maps by the model-based method developed by SAIC.
- Cross-validate group velocity maps obtained by the tomographic and model-based methods.
- Test and validate the maps and correction surfaces on IMS data at the CMR test bed.

### **REFERENCES**

Barmin, M.P., M.H. Ritzwoller, and A.L. Levshin (2001), A fast and reliable method for surface wave tomography, *Pure and Appl. Geophys.*, **158**, n.7, in press.

- Herrin, E. and T. Gofort (1977), Phase-matched filters: application to the study of Rayleigh waves, *Bull. Seismol. Soc. Am.*, **67**, 1259-1275.
- Levshin, A.L., L. Ratnikova, and J. Berger (1992), Peculiarities of surface wave propagation across central Eurasia, *Bull. Seismol. Soc. Am.*, **82**, 2464-2493.
- Levshin, A.L., M.H. Ritzwoller, and L.I. Ratnikova (1994), The nature and cause of polarization anomalies of surface waves crossing northern and central Eurasia, *Geophys. J. Int.*, **117**, 577-590.
- Levshin, A.L., M.H. Ritzwoller, and S.S. Smith (1996), Group velocity variations across Eurasia, *18th Seismic Research Symposium on Monitoring a CTBT, Proceedings*, 70-79.
- Levshin, A.L., M.H. Ritzwoller, L.I. Ratnikova, M. Silitch, R. Kelly, and B. O'Sullivan (1997), Intermediate period group velocity maps across Central Asia and parts of the Middle East, *19th Seismic Research Symposium on Monitoring a CTBT, Proceedings*, 67-76.
- Levshin, A.L., M.H. Ritzwoller, M.P. Barmin, A. Villaseñor, and C.A. Padgett (2001), New constraints on the Arctic crust and uppermost mantle: surface wave group velocities,  $P_n$ , and  $S_n$ , *Phys. Earth. Planet. Int.*, **123**, 185-204. Levshin, A.L. and M.H. Ritzwoller (2001), Automated detection, extraction, and measurement of regional surface waves, *Pure and Appl. Geophys.*, **158**, n.7, in press.
- Levshin, A.L., M.H. Ritzwoller, M.P. Barmin, and J.L. Stevens (2000), Assessing abilities to estimate short period group velocities in Central Asia, *22nd Annual DoD/DoE Seismic Research Symposium, Proceedings*, I, 67-76.
- Levshin, A.L. and M.H. Ritzwoller (2001), Discrimination, detection, depth, location and wave propagation studies using intermediate period surface waves in the Middle East, Central Asia, and the Far East, *Final Report on Contract DSWA01-97-C-0157*, DTRA.
- Ritzwoller, M.H., A.L. Levshin, S.S. Smith, and C.S. Lee (1995), Making accurate continental broadband surface wave measurements, *17th Seismic Research Symposium on Monitoring a CTBT, Proceedings*, 482-490.
- Ritzwoller, M.H., A.L. Levshin, L.I. Ratnikova, and D.M. Tremblay (1996), High resolution group velocity variations across Central Asia, *18th Seismic Research Symposium on Monitoring a CTBT, Proceedings*, 98-107.
- Ritzwoller, M.H. and A.L. Levshin (1998), Eurasian surface wave tomography: Group velocities, *J. Geophys. Res.*, **103**, 4839-4878.
- Ritzwoller, M.H., A.L. Levshin, L.I. Ratnikova, and A.A. Egorkin (1998), Intermediate period group velocity maps across Central Asia, western China, and parts of the Middle East, *Geophys. J. Int.*, **134**, 315-328.
- Stevens, J.L. and S.M. Day (1985), The physical basis for  $m_b:M_s$  and variable frequency magnitude methods for earthquake/explosion discrimination, *J. Geophys. Res.*, **90**, 3009-3020.
- Stevens, J.L. and K.L. McLaughlin (1997), Improved methods for regionalized surface wave analysis, *Maxwell Technologies Final Report*, submitted to Phillips Laboratory, MFD-TR-97-15887.
- Stevens, J.L. and K.L. McLaughlin (2001), Optimization of surface wave identification and measurement, *Pure and Appl. Geophys.*, **158**, n.7, in press.
- Villaseñor, A., M. H. Ritzwoller, A.L. Levshin, M.P. Barmin, E.R. Engdahl, W. Spakman, and J. Trampert (2001), Shear velocity structure of central Eurasia from inversion of surface wave velocities, *Phys. Earth. Planet. Int.*, **123**, 169-184. references